NÖHÜ Müh. Bilim. Derg. / NOHU J. Eng. Sci., 2022; 11(3), 813-818

Niğde Ömer Halisdemir Üniversitesi Mühendislik Bilimleri Dergisi
Niğde Ömer Halisdemir University Journal of Engineering Sciences

Araştırma makalesi / Research article

www.dergipark.org.tr/tr/pub/ngumuh / www.dergipark.org.tr/en/pub/ngumuh

$CdSO_4$-CdS Composite nanowires synthesized by arc discharge method

$CdSO_4$-CdS Kompozit nanotellerin ark deşarj yöntemi ile sentezi

Tugay Üstün[1,*], **Volkan Eskizeybek**[2], **Omar Toumiat**[3], **Ahmet Avcı**[4]

[1] *Başkent University, Kahramankazan Vocational School, 06980, Ankara, Turkey*
[2] *Çanakkale Onsekiz Mart University, Department of Materials Science and Engineering, 17100, Çanakkale, Turkey*
[3] *University of Constantine, Department of Pyhsics, 25000, Constantine, Algeria*
[4] *Necmettin Erbakan University, Department of Biomedical Engineering, 42090, Konya, Turkey*

Abstract

Herein, we successfully carried out the of CdS nanowires doped with $CdSO_4$ nanoparticles by arc discharge method. For this, two cadmium rods with high purity as anode and cathode electrodes were submerged in a liquid nitrogen medium. The cathode electrode was filled with micro-sized sulfur powder to synthesize CdS nanowires. CdS nanowires were obtained by oxidation using low temperature with $CdSO_4$ nanoparticles. After the arc discharge process, the resultant product was characterized to reveal structural and morphological properties. XRD and electron EDX analyses exposed the coexistence of the CdS and $CdSO_4$ phases. Scanning electron microscopy (SEM) investigations revealed that the synthesized nanostructures formed in a 1D wire nanostructure morphology with a diameter of less than 10 nm and several micrometers in length. Besides, the transmission electron microscopy (TEM) analysis was utilized to monitor the $CdSO_4$ nanoparticles located on CdS nanowires surface. It has been found that the absorption band blue-shifted with 0.53 eV. This blue shift originated from the quantum confinement in the nanoparticles.

Keywords: CdS, Nanowire, Arc-discharge, Photoluminescence

Öz

Bu çalışmada, $CdSO_4$ nanopartikülleri ile doplanmış CdS nanotellerinin sentezini ark deşarj yöntemi ile başarıyla gerçekleştirdik. Bunun için anot ve katot elektrotlar olarak yüksek saflıkta iki kadmiyum çubuk sıvı nitrojen ortamına daldırıldı. Katot elektrotu, CdS nanotellerini sentezlemek için mikro boyutlu kükürt tozu ile doldurulmuştur. CdS nanotelleri düşük sıcaklıkta oksitleme işlemi ile $CdSO_4$ nanoparçacıkları da elde edildi. Ark deşarj işleminden sonra, elde edilen ürün yapısal ve morfolojik özellikleri ortaya çıkarmak için karakterize edildi. X-Işını Kırınımı (XRD) ve elektron dağılımı spektroskopi (EDS) analizleri, CdS ve $CdSO_4$ fazlarının bir arada varlığını açıkça ortaya koymuştur. Taramalı elektron mikroskobu (SEM) incelemeleri, sentezlenmiş nanoyapıların 10 nm'den küçük bir çapa ve birkaç mikrometre uzunluğa sahip bir 1B tel nanoyapı morfolojisinde oluştuğunu ortaya çıkardı. Ayrıca, geçirimli elektron mikroskobu (TEM) analizi, CdS nanotellerinin yüzeyinde bulunan $CdSO_4$ nanopartiküllerini izlemek için kullanıldı. Absorpsiyon bandının maviye kaydığı 0.53 eV ile bulunmuştur. Bu maviye kayma, nanopartiküllerdeki kuantum sınırlamasından kaynaklandı.

Anahtar kelimeler: CdS, Nanotel, Ark deşarj, Fotolüminesans

1 Introduction

Metal-based nanostructures such as CdO, CdS, ZnS, and ZnO have become a crucial area of interest in nanotechnology due to their vital role in developing smart devices and functional materials in recent years. The most important physical properties of these materials were the carrier's spatial confinement and the discrete density of energy. These attractive physical properties enable tailoring their roles in engineering applications such as photocatalysis, luminescent materials, and light-emitting diodes (LEDs), and solar cells [1]. Among these nanostructures, cadmium sulfide (CdS) is considered a vital semiconductor with a bandgap in the visible range of 2.5 eV [2]. It has been reported that CdS nanostructures were sensitized into various nanocrystalline morphologies such as nanotubes [2], nanoparticles [3], nano-cluster [4], nanorods, and nano-spheres [5]. Due to advances in nanotechnology, the importance of one-dimensional nanoparticles, such as nanotubes, nanowires, and nanobelts, has increased in recent years. At most, the discovery of the room temperature excitonic laser emission in CdS nanowires at room temperature by Anlian et al. [5] and Agarwal et al. [6] paves the way to the laser sources with a low threshold. On the other hand, a promising way to efficient energy harvesting from solar light is the combination of nanomaterials properties to enhance the UV light absorption from solar light due to its broad bandgap (5.2 eV) and its relative facile ability to be obtained 1D nanostructure [7]. On the other hand, based on the synthesis method and process parameters, phase transition of CdS might occur, leading to the formation of CdO, $CdSO_4$, or complex CdO composites ($CdOSO_2$ and CdOs), which is notably affected by temperature and environment [8]. The presence of two or more phases enables CdS nanostructures to be tuned electrical properties, and in particular, to change their band gap. Furthermore,

---

* Sorumlu yazar / Corresponding author, e-posta / e-mail: tugayustun@baskent.edu.tr (T. Üstün)

Geliş / Recieved: 06.11.2020 Kabul / Accepted: 17.05.2022 Yayımlanma / Published: 18.07.2022
doi: 10.28948/ngmuh.820329

$CdSO_4$ is a well-known ionic crystal that has been used in thermoluminescent phosphors, gas sensors, electrolytes, and optical applications. As a result, producing self-assembled nanostructured semiconductors with different morphologies and complicated phase elements for further exploitation of their underlying photoelectric capabilities appears to be quite promising. In this work, we developed a facile synthesis method of CdS-$CdSO_4$ nanocomposites by a modified arc-discharge technique submerged in liquid nitrogen medium.

Arc-discharge (AD) in the liquid environment has been known as one of several methods to synthesize nanomaterials such as WO_3 [9], CuO [10] and CdO [11]. AD process submerged in a liquid medium has shifted an efficient nanostructures production technique with various vital benefits such as large-scale production, high efficiency, and cost-effectiveness. This technique particularly needs a dc power supply and an open vessel filled with a liquid medium. Like all other well-known techniques, it requires no vacuum environment, a high-temperature furnace, and reacting gases [11]. In this process, an electrical arc-discharge is formed between two highly pure crystalline metallic electrodes. The formed arc plasma evaporates the metal wires, and the evaporated matter is cooled in the liquid medium to produce nanomaterials through a self-assembling process.

In this study, we present the synthesis of CdS nanowires doped with $CdSO_4$ phase embedded on the nanowire surface by AD process submerged in liquid nitrogen environment. The resulting nanostructures were physically characterized to reveal their structural, morphological and optical properties.

2 Materials and methods

2.1 *Synthesis of cadmium sulfide nanowires*

Cd rods with diameters of 6 and 10 mm (99.99%) were employed and purchased from Alfa Aesar as anode and cathode electrodes. The chemical reactants have been of analytical grade and utilized as received.

Lab-made arc-discharge equipment was employed, as introduced in our previous works [12]. It consists of two cadmium electrodes with high purity. A cadmium rod with a 10 mm diameter and 20 mm length was used as the cathode. It was manufactured to have a smooth surface, wanted to retain uniform arc-discharge throughout the process. Anode electrode was machined from another cadmium rod with a 6 mm diameter and 60 mm in length. A 4 mm hole was machined in the anode and loaded with high purity sulfur powder. The arc current was provided (50 A, 20-30 V) by a direct current power supply. The arc discharge was started with the contact of electrodes. For a stable arc-discharge, the gap was controlled by measuring the voltage during the experiment. The products were transferred into de-ionized water. Following the settling process, the particles separated into two phases, one floating at the water's surface, the second precipitate at the bottom. The floating product was gathered on a silicon substrate and dried at 80 °C in the air, subsequently [13].

2.2 *Growth mechanism*

The coalescence of nanostructures is the most critical factor in the production of the CdS nanowires. During the arc discharge, pulverization of the Cd anode and sulfur powder occurred in the arc region, leading to the growth of nanoscale CdS according to the following Equation 1;

$$\begin{array}{lcl} Cd & \xrightarrow{\text{Heat and current}} & Cd^{+2} + 2e^{-} \\ S + 2e^{-} & \xrightarrow{\text{Heat and current}} & S^{-2} \\ Cd^{+2} + S^{-2} & \longrightarrow & CdS \end{array} \qquad (1)$$

The sharp temperature gradient from the arc zone to the liquid nitrogen medium plays a vital role in producing different nanoparticles with various morphologies [13]. In the hot plasma region, the formation of the molecular CdS may be more probable. These molecules are ejected from the hot plasma zone to the liquid nitrogen medium. At this time, these CdS molecules transfer their energy to the medium and condensed to form CdS nanoparticles, which is the critical process step for forming the nanowires. A similar phenomenon has been observed by [10] for $Cd(OH)_2$ nanowires addressing the oriented attachment of nanoparticles in nanowire morphology to reduced their total surface energy [14]. The coalescence may start with one particle acting as a seed for the nanowire's growth, as shown in Figure 2c. This growth phenomenon suggests the irreversible and perfectly aligned nanoparticles to form 1D nanostructures [15]. The complete oxidation of bulk CdS may have been achieved by according to following Equation 2;

$$CdS + 2O_2 \xrightarrow{O_2 \text{ flow } +80^{\circ}C} CdSO_4 \qquad (2)$$

As can be seen from Equation (2), the complete oxidizing of the bulk CdS only occurs under O_2 flow at high temperatures. However, the oxidation occurs even at low temperature (80 °C) and inadequate oxygen amount due to the comparatively smaller particle size and high mismatch between the assembled particles in our case (Figure 2d). As a result, these conditions may become favorable to the $CdSO_4$ phase formation as the XRD pattern, and EDS analysis confirms it. Also, the different contrasted regions in Figure 2b may be attributed to the $CdSO_4$ nanoparticles embedded in the CdS nanowire.

2.3 *Characterization*

The obtained products were dispersed in alcohol ultrasonically for morphological and structural examinations. X-ray diffraction (XRD) spectrum was obtained on Shimadzu XRD-6000. The diffractometer was performed at 0.15405 nm CuKα radiation. Scanning electron microscopy (SEM) and energy-dispersive X-ray spectrometry (EDS) analyses were carried out by JEOL/JSM6335F-EDS SEM. Transmission electron microscopy (TEM) and selected area electron diffraction (SAED) patterns were taken by a JEOL 2100 HRTEM at 300 kV. The optical properties were examined using an Ocean Optics HR4000 UV–VIS–NIR spectrophotometer equipped with xenon and deuterium lamps. The fluorescence emissions were obtained with a Perkin Elmer LS 50 B spectrometer with an optical way of 1 cm, at room temperature, and 0.2 g/L concentration in ethanol solution.

3 Result and discussion

3.1 Morphology

Figure 1a shows a typical SEM image of CdS nanowires. As seen, the obtained nanostructures are in the nanowire form while they are in entangled form in bundles. The nanowires have a regular diameter of 10 nm, and their length is up to several micrometers. It is seen in Figure 1b that there is no other morphology rather than the nanowire form, which shows the effectiveness of the production technique to synthesize uniform nanostructures [12].

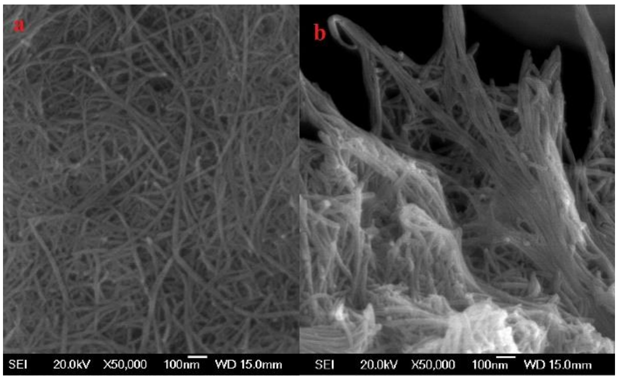

Figure 1. SEM images of the as prepared nanocomposites showing mean diameter around 10 nm of the obtained nanowire with several micrometer in length (a) Homogenous field and (b) Nanowire form in entangled form in bundles.

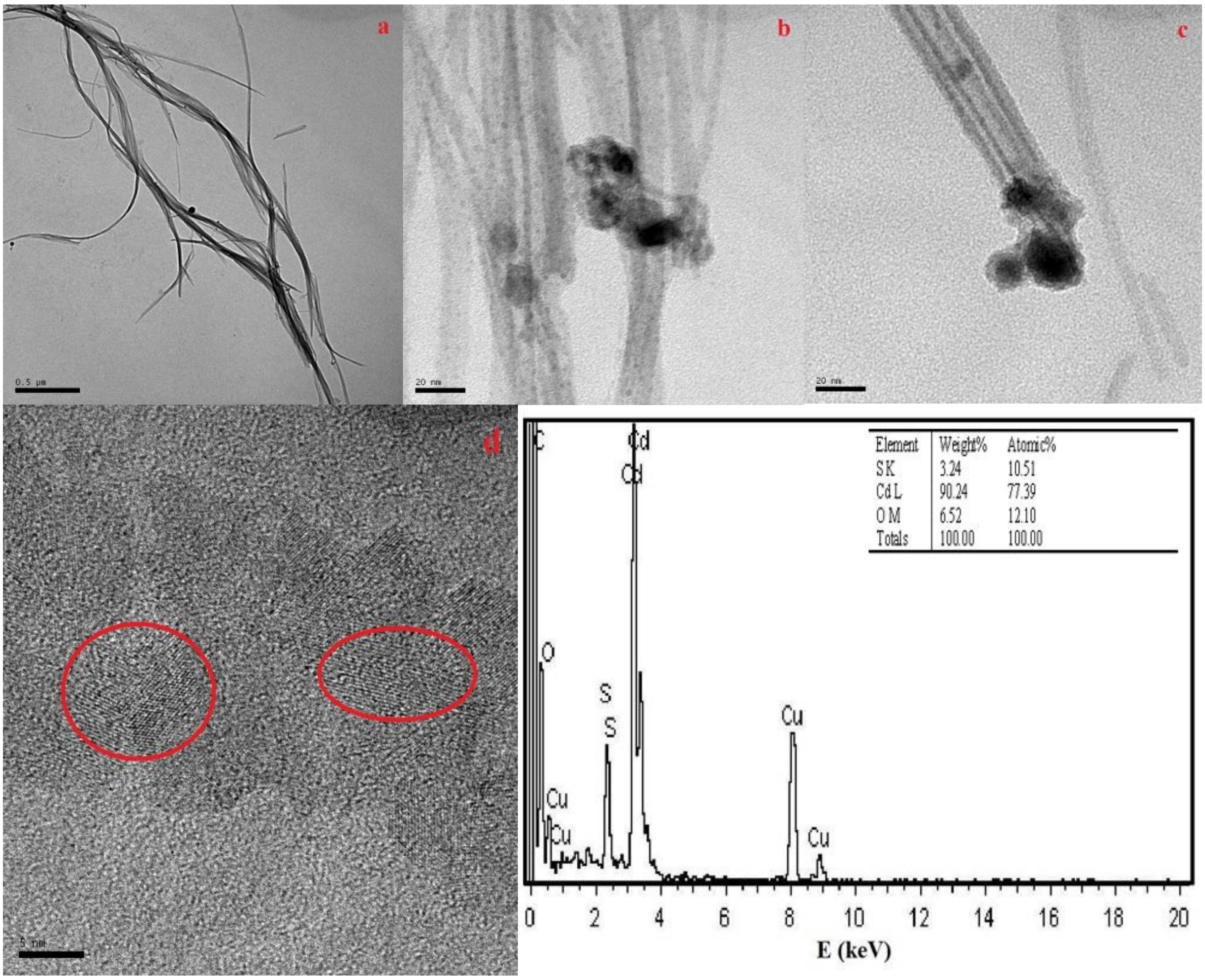

Element	Weight%	Atomic%
S K	3.24	10.51
Cd L	90.24	77.39
O M	6.52	12.10
Totals	100.00	100.00

Figure 2. TEM images of the nanocomposite (a) nanowire structures (b) high magnification of the corresponding nanowire structures with embedded Q dots (diameter about 5 nm) (c) monitoring a nanowire with nanoparticles at the tip, which may act as a seed (d) high resolution TEM image of a polycrystalline nanowire showing the well-crystallized nanoparticles. The scale bars are 0.5 µm, 20 nm, 20 nm and 5 nm for (a), (b), (c) and (d) respectively (e) energy dispersive spectra of nanocomposite showing only the presence of oxygen, Cd and S with the atomic ratios of elements.

The TEM images of the nanocomposite are presented in Figure 2. Figure 2a presents the nanowire morphology of the resultant nanocomposite with a mean diameter of around 10 nm and several micrometers in length. This observation is in good agreement with FE-SEM results. In Figure 2b, the high-resolution TEM (HRTEM) image is presented. The image exhibits the presence of small nanoparticles, with different contrast embedded on the nanowire. This figure also reveals a hexagonal-shaped nanostructure at the tip of the nanowire with the same contrast. In particular, HRTEM image of the tip of one nanowire presented in Figure 2c exhibits a nearly hexagonal-shaped nanoparticle with the same diameter as the nanowire. Similarly, the HRTEM image of a portion of the nanowire (Figure 2d) shows the nanowire's polycrystalline nature, with well-crystallized nanoparticles assembled with different crystalline orientations. Similar observations have been reported elsewhere [11] for the Cd(OH)$_2$ nanowires, where most of the nanoparticles coalesced and formed the CdS nanowire. We confidently believe that the nanowire morphology is not smooth due to this formation mechanism. This observation may be useful in increasing the specific surface of the obtained nanocomposite. Moreover, EDS shows only the presence of oxygen, sulfur, and cadmium in our samples in excellent agreement with XRD results, as shown in Figure 2e. The carbon and copper peaks in the EDS spectrum arise from the carbon coating and copper grid used for TEM sample preparation.

3.2 *Structural properties*

The XRD pattern of the as-synthesized nanostructures is illustrated in Figure 3. The XRD pattern reveals the presence of CdS as a major phase due to the sharp peaks of hexagonal wurtzite CdS (JCPDS 41-1049) structure with lattice parameters as a=b=4.12 Å and c=6.68 Å. The diffraction peaks at 2θ=24.95, 26.62, 28.36, 36.78, 43.85, 48.03, and 52.06 are attributed to (100), (002), (101), (102), (110), (103) and (112) planes of hexagonal CdS nanostructures. In addition, CdSO$_4$ (JCPDS 85-0673) nanostructures as a minor phase are also identified with cell parameters as a= 4.71 Å and b = 6.55 Å addressing the orthorhombic space group Pn21m.

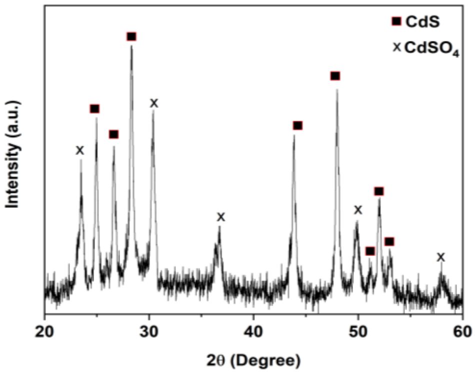

Figure 3. XRD pattern of the prepared nanocomposite presenting the coexistence of two phases; hexagonal CdS and orthorhombic CdSO$_4$

The diffraction peaks at 2θ=23.51, 30.38, 38.2 and 49.83 can be indexed to (101), (111), (112) and (002) planes of CdSO$_4$ nanostructures. However, it is apparent from figure that CdSO$_4$ phase represents peak broadening compared to CdS phase. This peak broadening indicates the nanometer scaled grain size of the CdSO$_4$ phase, which indicates that the mean grain size of the CdSO$_4$ phase is comparatively small. According to the Scherer formula, the calculated mean crystalline size is 2-10 nm. A probable formation of this phase can be due to the diffusion of oxygen in the sulfur vacancies sites of CdS matrix. The surface of CdS nanowires possess rich vacancies due to the rapid synthesis process, which causes a high internal stress in the lattice. Therefore, after the CdS nanowire formation, CdSO$_4$ nanoparticles are formed with the oxygen diffusion in the sulfur vacancies on the surface of nanowires. At the same time, the relaxation of the lattice is achieved.

3.3 *Optical properties*

Figure 4 presents the optical absorption spectra of CdS-CdSO$_4$ nanowires. Two characteristics are apparent from this spectrum: discrete excitonic absorption broadband and a shift of the excitonic absorption band towards a lower wavelength than bulk CdS. The increase in absorption at lower wavelengths is attributed to the electron-hole photogeneration. Furthermore, the excitonic absorption is evident, revealing a visible increase in bandgap energy. The increment in the bandgap energy (~0.53 eV) can be related to the reduction in nanowires' average diameter and CdSO$_4$ nanoparticles existence as the second phase on the nanowire. The theoretical explanation addressing the bandgap increase based on quantum confinement is given by [16];

$$E_g \approx E_{g0} + (h^2\pi^2\mu/2d^2) - (1.8e^2/\varepsilon d) \qquad (3)$$

Eg$_0$ is the energy gap for bulk material, i.e., 2.45 eV, d is the mean grain size, μ is the exciton effective mass, and ε is the dielectric constant. For CdS, μ = 0.18 m0, and ε = 8.58. This formulation can be employed to estimate the increase in the bandgap energy when the grain size reaches the nanowire's diameter. The estimation yields a value of 0.04 eV, notably different from the obtained value of 0.53 eV. The estimated mean grain size giving the exact shift value was 6-7 nm, which was closed to the measured value of the nanoparticles' mean diameter. Based on these results, the bandgap shift is governed by the absorption of the CdSO$_4$ phase. However, substantial quantum confinement is presumed to occur in CdSO$_4$ nanoparticles with a grain size of around 2.4 nm in the order of the exciton Bohr radius [16]. Additional impacts responsible for bandgap shift are strain, crystallinity [17], and exciton longitudinal optical phonon interaction [5].

The photoluminescence spectrum of the CdS-CdSO$_4$ nanocomposite is given in Figure 5. As seen in the figure, there is a robust and broad luminescence band around 2.2 eV, which may be related to the defect emission in CdS. The other band located 2.8 eV is assigned to the band-to-band emission of CdS. The change in PL emissions can be explained with the crystal defects triggered by the $CdSO_4$ nanoparticles existence as the second phase on the nanowire.

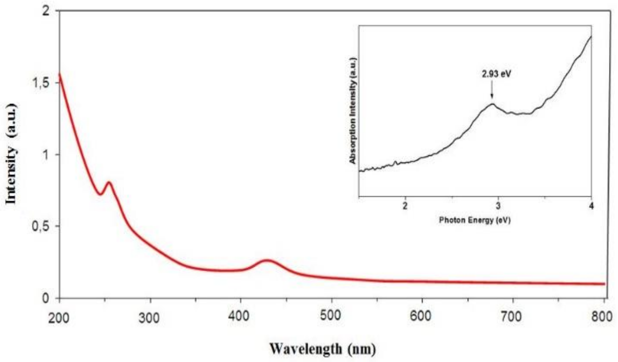

Figure 4. UV-Visible absorption spectra of CdS-$CdSO_4$ nanocomposite presenting a broad band

The $CdSO_4$ phase In comparison to the CdS sample, the absorption edge of the $CdSO_4$ phase shifts to a higher wavelength [18]. Banerjee et al. [19] reported the size induced phase transformation of CdS nanoparticles, indicating that the deformation fault configuration is responsible for the structural transition. This phenomenon occurs by slipping one part of the crystal past another, parallel to the close-packed basal planes of the hexagonal unit cell of CdS.

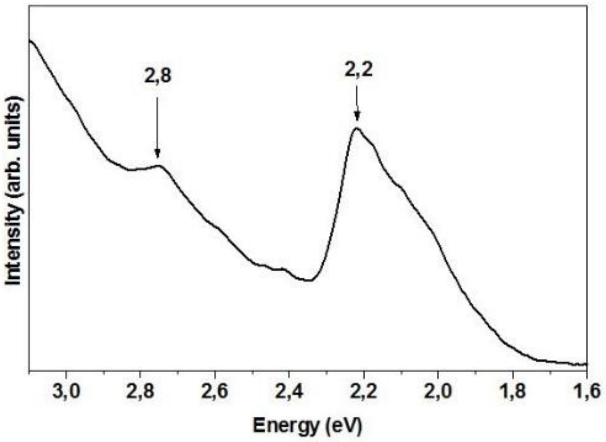

Figure 5. Photoluminescence spectrum of the prepared nanocomposite showing a broad luminescence band around 2.2 eV related to defect emissions and band around 2.8 eV that is attributed to the band-to-band emission of CdS

4 Conclusions

In summary, CdS-$CdSO_4$ nanomaterials have been synthesized by the arc discharge process followed by heating at 80 °C in air. The bulk CdS nanowires transform to $CdSO_4$ by oxidation under the suitable temperature and atmosphere. The XRD pattern of CdS-$CdSO_4$ nanomaterials confirm to $CdSO_4$ nanoparticles embedded in the CdS nanowire. CdS nanowire shows the hexagonal crystal structure while $CdSO_4$ nanoparticles present an orthorhombic crystal structure. Also, the high magnification TEM revealed the embedded $CdSO_4$ nanoparticles at the CdS nanowires surface. These nanocomposites exhibit a substantial blue shift ~0.5 eV due to nanoparticle absorption. This optical behavior may be due to the UV absorption of nanoparticles and the nanowires visible absorption. The synthesized nanocomposite is suitable for optoelectronic device, sensors and photocatalysis applications.

Conflicts of interest

No conflict of interest was declared by the authors.

Similarity rate (iThenticate): 17%

References

[1] S. Yuvaraj, A. C. Fernandez, M. Sundararajan, C. S. Dash, and P. Sakthivel, Hydrothermal synthesis of ZnO–CdS nanocomposites: Structural, optical and electrical behavior. Ceram. Int., 46(1), 391–402, 2020. https://doi.org/10.1016/j.ceramint.2019.08.274.

[2] A. Pan et al., Stimulated emissions in aligned CdS nanowires at room temperature. J. Phys. Chem. B, 109(51), 24268–24272, 2005. https://doi.org/10.1021/jp055164m.

[3] M. Salavati-Niasari, F. Davar, and M. R. Loghman-Estarki, Long chain polymer assisted synthesis of flower-like cadmium sulfide nanorods via hydrothermal process. J. Alloys Compd., 481(2), 776–780, 2009. https://doi.org/10.1016/j.jallcom.2009.03.086.

[4] R. Agarwal, C. J. Barrelet, and C. M. Lieber, Lasing in single cadmium sulfide nanowire optical cavities. Nano Lett., 5(5), 917–920, 2005. https://doi.org/10.1021/nl050440u.

[5] G. Nagaraju, S. Ashoka, C. N. Tharamani, and G. T. Chandrappa, A facile low temperature hydrothermal route to CdSO4 nanotubes/rods. Mater. Lett., 63(3), 492–495, 2009. https://doi.org/10.1016/j.matlet.2008.11.032.

[6] T. Üstün, V. Eskizeybek, and A. Avcı, Selectively Nanocube Formation of Tungsten Oxide (WO 3). Celal Bayar Univ. J. Sci., 16(2), 149–153, 2020. https://doi.org/10.18466/cbayarfbe.677407

[7] T. Üstün, V. Eskizeybek, and A. Avcı, CuO Nanoparçacıkların Kolay ve Amorf Yapıda Sentezi. Konya J. Eng. Sci., 7(4), 696–704, 2019. https://doi.org/10.36306/konjes.654449.

[8] Z. Li, F. Davar, J. Chen, Z. Li, and X. Fang, CdS/CdSO4 nanoflower-based photodetector with enhanced photoelectric performances. ACS Applied Nano Materials, 3(10), 10190-10199, 2020. https://doi.org/10.1021/acsanm.0c02166.

[9] V. Eskizeybek, A. Avcı, and M. Chhowalla, Structural and optical properties of CdO nanowires synthesized from Cd(OH)2 precursors by calcination. Cryst. Res. Technol., 46(10), 1093–1100, 2011. https://doi.org/10.1002/crat.201100221.

[10] V. Eskizeybek, O. Demir, A. Avci, and M. Chhowalla, Synthesis and characterization of cadmium hydroxide nanowires by arc discharge method in de-ionized water.

J. Nanoparticle Res., 13(10), 4673–4680, 2011. https://doi.org/10.1007/s11051-011-0430-z.

[11] V. Eskizeybek, E. S. Karabulut, and A. Avci, Synthesis of carbon nanostructures and CaCO3 nanoparticles by arc discharge in mineral water. J. Nano Res., 15, 57–67, 2011. https://doi.org/10.4028/www.scientific.net/JNanoR.15.57.

[12] T. Charinpanitkul, N. Sano, P. Muthakarn, and W. Tanthapanichakoon, Enhancing effect of monoolein surfactant on carbon nanoparticle synthesis by arc discharge in liquid. Mater. Res. Bull., 44(2), 324–327, 2009. https://doi.org/10.1016/j.materresbull.2008.05.017.

[13] N. Sano et al., Properties of carbon onions produced by an arc discharge in water. J. Appl. Phys., 92(5), 2783–2788, 2002. https://doi.org/10.1063/1.1498884.

[14] M. Ye, H. Zhong, W. Zheng, R. Li, and Y. Li, Ultralong cadmium hydroxide nanowires: Synthesis, characterization, and transformation into CdO nanostrands. Langmuir, 23(17), 9064–9068, 2007. https://doi.org/10.1021/la070111c.

[15] D. F. Zhang, L. D. Sun, J. L. Yin, and C. H. Yan, Low-temperature fabrication of highly crystalline SnO2 nanorods. Adv. Mater., 15(12), 1022–1025, 2003. https://doi.org/10.1002/adma.200304899.

[16] D. Redfield and W. J. Burke, Optical absorption edge of LiNbO3. J. Appl. Phys., 45(10), 4566–4571, 1974. https://doi.org/10.1063/1.1663089.

[17] R. Venugopal, P. I. Lin, C. C. Liu, and Y. T. Chen, Surface-enhanced Raman scattering and polarized photoluminescence from catalytically grown CdSe nanobelts and sheets. J. Am. Chem. Soc., 127(32), 11262–11268, 2005. https://doi.org/10.1021/ja044270j.

[18] S. Yılmaz, İ. Polat, M. A. Olgar, M. Tomakin, S. B. Töreli, and E. Bacaksız, Physical properties of CdS: Ga thin films synthesized by spray pyrolysis technique. Journal of Materials Science: Materials in Electronics, 28(4), 3191-3199, 2017.

[19] R. Banerjee, R. Jayakrishnan, and P. Ayyub, Effect of the size-induced structural transformation on the band gap in CdS nanoparticles. Journal of Physics: Condensed Matter, 12(50), 10647, 2000.